



HAL
open science

3D finite element simulation of TIG weld pool

X. Kong, Olivier Asserin, S. Gounand, P. Gilles, J.-M. Bergheau, M. Médale

► **To cite this version:**

X. Kong, Olivier Asserin, S. Gounand, P. Gilles, J.-M. Bergheau, et al.. 3D finite element simulation of TIG weld pool. IOP Conference Series: Materials Science and Engineering, 2012, MCWASP XIII - International Conference on Modeling of Casting, Welding and Advanced Solidification Processes, 33, pp.012025. 10.1088/1757-899X/33/1/012025 . cea-02284855

HAL Id: cea-02284855

<https://cea.hal.science/cea-02284855>

Submitted on 3 Jun 2021

HAL is a multi-disciplinary open access archive for the deposit and dissemination of scientific research documents, whether they are published or not. The documents may come from teaching and research institutions in France or abroad, or from public or private research centers.

L'archive ouverte pluridisciplinaire **HAL**, est destinée au dépôt et à la diffusion de documents scientifiques de niveau recherche, publiés ou non, émanant des établissements d'enseignement et de recherche français ou étrangers, des laboratoires publics ou privés.

3D finite element simulation of TIG weld pool

X Kong^{1,2,3}, O Asserin¹, S Gounand¹, P Gilles², JM Bergheau³ and M Medale⁴

¹CEA, DEN, DANS, DM2S, F-91191 Gif-sur-Yvette, France

²AREVA NP, Paris La Défense, France

³LTDS, Ecole Nationale d'Ingénieurs de Saint-Etienne, France

⁴Ecole Polytechnique Universitaire de Marseille, Marseille, France

E-mail: xiaofei.kong@enise.fr, olivier.asserin@cea.fr

Abstract. The aim of this paper is to propose a three-dimensional weld pool model for the moving gas tungsten arc welding (GTAW) process, in order to understand the main factors that limit the weld quality and improve the productivity, especially with respect to the welding speed. Simulation is a very powerful tool to help in understanding the physical phenomena in the weld process. A 3D finite element model of heat and fluid flow in weld pool considering free surface of the pool and traveling speed has been developed for the GTAW process. Cast3M software is used to compute all the governing equations. The free surface of the weld pool is calculated by minimizing the total surface energy. The combined effects of surface tension gradient, buoyancy force, arc pressure, arc drag force to drive the fluid flow is included in our model. The deformation of the weld pool surface and the welding speed affect fluid flow, heat flow and thus temperature gradients and molten pool dimensions. Welding trials study is presented to compare our numerical results with macrograph of the molten pool.

1. Introduction

Gas tungsten arc welding (GTAW) is a widely used technique for joining steel in nuclear industry where the weld quality must be ensured. An increased productivity of welding would have a very important economic impact for the industrial sector. Although GTAW is already a very efficient process, it can be improved, especially with respect to the welding speed. The aim of this paper is to propose a three-dimensional weld pool model for the moving GTAW process, in order to understand the main factors that limit the weld process and improve the productivity. Simulation is very helpful in understanding the physical phenomena in the weld pool and optimizing the process. In the recent years, many research dealing with the simulation of welding processes have been carried out and great progress has been made. Tanaka [1] took into account tungsten cathode, arc plasma and anode in a 2D axisymmetric unified model, but the deformation of the free surface of weld pool isn't taken into account. Debroy and al. [2] developed a 3D model with a moving heat source but the Marangoni coefficient is assumed constant. Lu and al. [3] developed a coupled model in 2D axisymmetric with the interface deformation, and the weld pool shape calculated agrees better with the experiment than the model without the free surface. Wu and al. [4] studied both front and back side deformations of fully penetrated GTAW weld pool surfaces, they gave a detailed derivation of the partial differential equation for predicting both surface deformation. Kim and Na [5] presented a 3D quasisteady heat and fluid flow analysis for the moving heat source of the gas metal arc welding

(GMAW) process with the free surface, and Hu and al. [6] modelled the transient weld pool dynamics under the periodic impingement of filler droplets. However, there is no impingement of droplets in GTAW which is very different from GMAW. Most of the present mathematical model are realised with the method of finite volume or finite difference, nowadays there is a increasing tendency to apply finite element methods. Among the reasons can be ability of the finite element method to handle complex coupled thermomechanical mechanisms with various and complex boundary conditions.

In this paper, a 3D finite element model considering free surface, moving source and temperature dependence of thermophysical properties for the GTAW is performed. The free surface profile is calculated by minimizing the total energy of the surface, the arc pressure, the arc drag force and the heat flux are given by a 2D axisymmetric arc plasma unified model [7]. The continuity equation, momentum equation and energy conservation equation are solved together by the Cast3M software [8], until a steady solution is found. The calculated GTAW weld bead geometry shows favourable agreement with experimental results.

2. Mathematical model

The 3D model of the welding pool with taking into account the traveling speed and the free surface is shown below. The assumptions are the following:

- a stationary solution is sought;
- the liquid metal is considered a Newtonian fluid;
- it is assumed that the flow of liquid metal is not turbulent;
- it is assumed that the Boussinesq approximation can be used;
- the speed of the power source v_s is assumed constant and the equations are solved in a reference frame moving with the source;
- in the fluid phase, the equations of conservation of mass, momentum and energy are solved, only the energy equation remains in the solid phase.

The unknowns of the problem are:

- \mathbf{v} velocity in the fluid phase in the reference frame linked to the source ($\mathbf{v} = \mathbf{v}_s$ in the solid phase);
- p , the pressure in the fluid phase;
- h and T , the enthalpy and the temperature.

2.1. Continuity equation

In the weld pool region, the continuity equation for an incompressible fluid holds:

$$\nabla \cdot \mathbf{v} = 0 \quad (1)$$

where v is the velocity of the fluid in the weld pool.

2.2. Momentum equation

The flow of the liquid metal in the weld pool conforms to the following equations:

$$\rho(\nabla \mathbf{v}) \cdot (\mathbf{v} - \mathbf{v}_s) = -\nabla p + \nabla \cdot \mu(\nabla \mathbf{v} + \nabla^T \mathbf{v}) + \mathbf{f}_{\text{Bou}} + \mathbf{f}_{\text{Ext}} \quad (2)$$

$$\rho = \rho_0 + \frac{\partial \rho}{\partial T}(T - T_{ref}) \quad (3)$$

where \mathbf{v}_s is the velocity of the power source, p is the hydrostatic pressure, μ is the viscosity, the buoyancy force: $\mathbf{f}_{\text{Bou}} = \rho_0 \mathbf{g} \beta (T - T_{ref}) \mathbf{u}_z$ where ρ_0 is the mass density at the temperature

$T_{ref} = 1730K$ and u_z is a vertical unit vector, the force of extinction speed: $\mathbf{f}_{Ext} = -AF_s(T)\mathbf{v}$ avec $A = 10^{12} \gg 1$ where F_s is the solid fraction [9].

The boundary conditions are :

$$\mathbf{v} = \mathbf{v}_s \text{ at } \partial\Omega_{s/l} \quad (4)$$

$$\mathbf{v} \cdot \mathbf{n} = 0 \text{ at } \partial\Omega_f \quad (5)$$

$$(\mu(\nabla\mathbf{v} + \nabla^T\mathbf{v}) \cdot \mathbf{n}) \cdot \mathbf{t} = \mathbf{f}_{Marangoni} \cdot \mathbf{t} + \mathbf{f}_{drag} \cdot \mathbf{t} \text{ at } \partial\Omega_f \quad (6)$$

where $\partial\Omega_{s/l}$ represent the liquid/solid interface and $\partial\Omega_f$ is the free surface, \mathbf{n} and \mathbf{t} are the normal and the tangential direction to surface, \mathbf{f}_{drag} is the arc drag force which will be given in the next subsection as a kind of surface source, $\mathbf{f}_{Marangoni} = \frac{\partial\gamma}{\partial T}\nabla T$, $\frac{\partial\gamma}{\partial T}$ is given by

$$\frac{\partial\gamma}{\partial T} = -A_r - R\Gamma_s \ln(1 + k_1 a_s \exp(-\Delta H_0/RT)) - \frac{k_1 a_s \Gamma_s \Delta H_0 \exp(-\Delta H_0/RT)}{(1 + k_1 a_s \exp(-\Delta H_0/RT))T} \quad (7)$$

where γ_m is the surface tension at melting temperature, A_r is the opposite of $d\gamma/dT$ for a pure FeS alloys, R is the gas constant, Γ_s is the surface excess at saturation, a_s is the activity of sulfur, ΔH_0 is the standard heat of adsorption, and k_1 is a constant related to entropy of segregation [10].

2.3. Energy conservation equation

The energy conservation can be written as follows :

$$\rho c_p (\nabla h) \cdot (\mathbf{v} - \mathbf{v}_s) = \nabla \cdot \lambda \nabla T \quad (8)$$

where c_p is the specific heat, h is the enthalpy, λ is the thermal conductivity.

The boundary conditions are :

$$h = h_0 \text{ on } \partial\Omega_{in} \quad (9)$$

$$\lambda \nabla T \cdot \mathbf{n} = 0 \text{ on } \partial\Omega_{out} \quad (10)$$

$$\lambda \nabla T \cdot \mathbf{n} = q_r + q_c + q_s \text{ on } \partial\Omega_{surf} \quad (11)$$

where $\partial\Omega_{in}$ and $\partial\Omega_{out}$ are the surface entering and leaving of the calculated domain, $\partial\Omega_{surf}$ represent the other surfaces of the workpiece. The convective heat loss is $q_c = -h_c(T - T_\infty)$, and the radiative loss is $q_r = -\epsilon\sigma(T^4 - T_\infty^4)$, q_s is the heat flux which will be given in the next subsection.

2.4. The free surface

The surface depression will form a shape which minimizes the total energy. The total energy to be minimized includes the surface energy due to the change in area of the pool surface, the potential energy in the gravitational field and the the work performed by the arc pressure displacing the pool surface [4].

$$\frac{\gamma}{R} = \rho_0 \mathbf{g} \varphi + P_a + \lambda \quad (12)$$

R and φ are the radius curvature and the elevation, φ is the elevation, γ represent the surface tension which is a variable in function of temperature. λ is the Lagrange multiplier which can be determined from keeping constant volume of the workpiece. The surface tension depends on temperature, for FeS alloys, following the model presented by Sahoo et al [10] γ is :

$$\gamma = \gamma_m - A_r(T - T_f) - RT\Gamma_s \ln(1 + k_1 a_s \exp(-\Delta H_0/RT)) \quad (13)$$

P_a is the arc pressure distribution at the free surface which will be given in the next subsection.

2.5. Treatment of latent heat

In order to treat phase change in the weld pool liquid/solid interface, the method of V.R. Voller [9], [11] is used. The total enthalpy H is represented as the integral of heat capacity with respect to temperature and can be written as follows:

$$H(T) = \int_{T_{ref}}^T \rho c_p(T) dT \quad (14)$$

where $\rho c_p(T)$ is the volumetric heat capacity which depends on temperature, and where T_{ref} is a reference temperature. In the industrial application, it is assumed that the phase change takes place over a finite interval $[T_s, T_l]$, the enthalpy function can be given by:

$$H(t) = \begin{cases} \int_{T_{ref}}^T \rho c_s(T) dT, & \text{for } T \leq T_s, \\ \int_{T_{ref}}^{T_s} \rho c_s(T) dT + \int_{T_s}^T \rho \frac{\partial L}{\partial T} dT, & \text{for } T_s < T \leq T_l, \\ \int_{T_{ref}}^{T_s} \rho c_s(T) dT + \rho L + \int_{T_l}^T \rho c_l(T) dT, & \text{for } T > T_l, \end{cases} \quad (15)$$

where T_s and T_l are the solidus and liquidus temperatures, and $\rho c_s(T)$ and $\rho c_l(T)$ are the temperature dependent volumetric heat capacities, L is latent heat.

2.6. Thermophysical properties

The temperature dependence of thermophysical properties is considered in this paper instead of supposing constant values. The thermophysical properties in solid and liquid ($c_p, h, \rho, \lambda, \mu, \beta$) for the material 316L steel are taken from Kim [12], for $\frac{\partial \gamma}{\partial T}$ and γ , the formula of Sahoo [10] is used. Other thermophysical properties and parameters used in this paper are summarized in Table 1.

2.7. Determination of surface sources

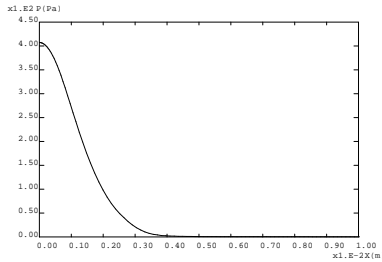
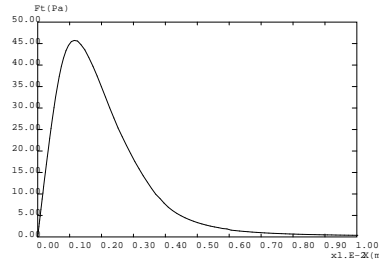
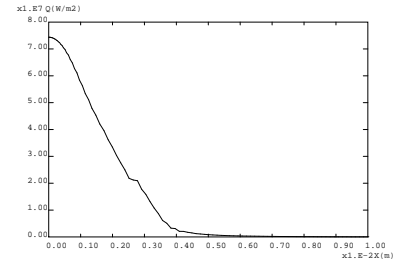
The study focusses on the weld pool behaviour, classical Gaussian distribution for the heat flux and arc pressure could have been used. However, this would have affected the simulation predictive capabilities, because the parameters of Gaussian distribution are not related to the welding operating parameters. So an hybrid 2D-3D approach is performed: the boundary conditions used in the three-dimensional weld pool model (heat flux, arc pressure and arc drag force) are calculated with a 2D axisymmetric arc plasma model [7]. The present GTAW experiment are carried out under following conditions: 316L steel workpiece with dimensions $200 \times 50 \times 6 \text{ mm}^3$, the welding current is 150 A, the arc voltage is 10 V, the arc length is 2 mm, the welding speed is 15 cm/min, the shielding gas is argon with flow rate 20 l/min, the tungsten electrode is of diameter 3.2 mm with tip angle 30° . Then these welding conditions are used in the 2D axisymmetric arc plasma model, figures 1, 2 and 3 show the 2D-computed heat flux, arc pressure and arc drag force which will be used in the 3D finite element weld pool model.

3. Numerical model

The finite element method is used to discretize the equations of the problem. Quadratic and linear finite elements are used for the variable \mathbf{v} and for the variables p, h and T . The method of weighted residuals is applied to seek the cancellation of integral terms associated with our problem. The coupling between the problem of fluid flow and heat transfer is taken into account with a suitable algorithm for solving the uncoupled finite element formulation (Table 2). The system of equations to be solved is non-linear, it is found that the thermal non-linearities are resolved fairly with the enthalpy formulation used, but the non-linearities associated with the

Table 1. Thermophysical properties of 316 stainless steel and welding conditions

Nomenclature	Symbol	Value (unit)
Sulfur activity	a_s	0.03 wt.%
Negative of $\frac{d\gamma}{dT}$ for pure metal	A_γ	$4.3 \times 10^{-4} N.m^{-1}K^{-1}$
Gas constant	R	$8314.3 J.kg^{-1}.mol^{-1}.K^{-1}$
Surface tension at melting temperature	γ_m	$1.27 N.m^{-1}$
Constant related to entropy of segregation	k_1	0.00318
Surface excess at saturation	Γ_s	$1.3 \times 10^{-8} kg.mol.m^{-2}$
Convection coefficient	h_c	$80 W.m^2.K^{-4}$
Radiation emissivity	ϵ	0.4
Latent heat of fusion	L	$2.47 \times 10^{-5} J.kg^{-1}$
Solidus temperature	T_s	1670 K
Liquidus temperature	T_l	1730 K
Ambient temperature	T_∞	293 K
Welding voltage	U	10 V
Welding current	I	150 A
Welding speed	v_s	$2.10^{-3} m.s^{-1}$
Maximum arc pressure	P_{max}	407 Pa
Thickness of workpiece	H_w	$6.10^{-3} m$
Width of workpiece	W_w	$5.10^{-2} m$
Length of workpiece	L_w	$2.10^{-1} m$

**Figure 1.** Radial evolution of arc pressure [7].**Figure 2.** Radial evolution of arc drag force [7].**Figure 3.** Radial evolution of heat flux [7].

fluid are generally more difficult to treat, for example the non-linearities due to the convective term and the phase change. The strategy is as follows: at the beginning of the calculation, the driving force $\mathbf{f}_{\text{Marangoni}}$ is initialized to zero, the thermal problem is solved. When there is a convergence on the unknowns of the non-linear problem, the intensity of the driving force f_α is increased with a coefficient α . And for improving the convergence, the convection terms are upwinded using a Streamline-Diffusion method.

Table 2. Algorithm for solving the non-linear problem

Initial condition: $(\mathbf{v}, p, h, T, \alpha)^0$ at $i = 0$
Repeat
$i = i + 1$
Determination of the fluid mesh
Calculation of the increments $\delta\mathbf{v}, \delta p$ and update $(\mathbf{v}, p)^i = (\mathbf{v}, p)^{i-1} + (\delta\mathbf{v}, \delta p)$
Calculation of the free surface profile, update $\varphi^i = \varphi^{i-1} + \delta\varphi$ and mesh movement
Calculation of the increment δh , update $h^i = h^{i-1} + \delta h$ and calculation $T^i = T(h^i)$
when $\delta_{inc} = (\delta\mathbf{v}, \delta p, \delta h) < \delta_{conv}$, $\alpha = \min(\alpha * f_\alpha, 1)$
until $\delta_{inc} < \delta_{conv}$ and $\alpha = 1$

4. Results and discussion

Figure 4 show the temperature and velocity field with heat transfer and fluid flow model taking into account the free surface, as shown in this figure, the base metal ahead of the heat source has not yet melted. The weld top surface of the region directly under the heat source is strongly deformed under the arc pressure, the molten metal is pushed to the rear part of the weld pool by combined effect of all the driving forces. As the monitoring location moves away from the heat source, the weld pool surface shows less depression because of reduction of arc pressure. Furthermore, the accumulation of the liquid metal in the rear part is clearly shown.

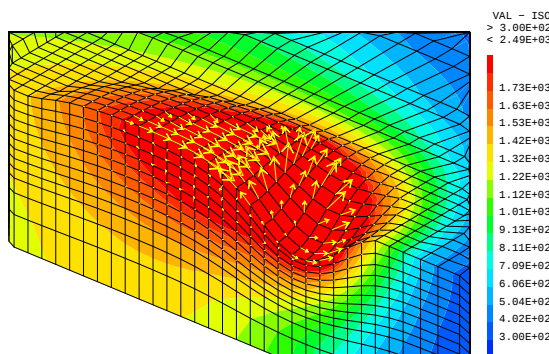


Figure 4. Calculated weld pool with considering free surface.

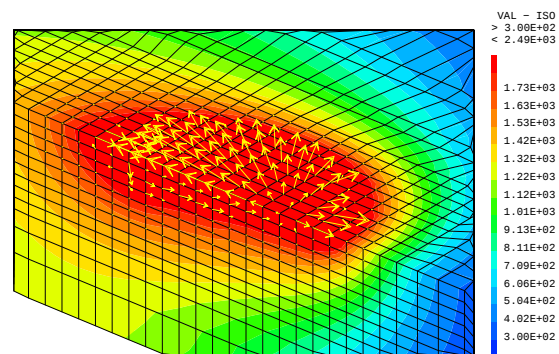


Figure 5. Calculated weld pool without considering free surface.

4.1. Weld temperature and fluid velocity field

In order to understand the influence of the free surface on the weld temperature and fluid velocity, two simulations are performed using the experimental welding parameters: one takes into account the free surface in our model (figure 4) and the other one doesn't (figure 5). Table 3 summarize the calculated weld pool characteristics, the maximal temperature in the case without free surface is 220 K higher than the one with free surface. When the free surface is taken into account, the fluid velocity is increased by the depression of free surface, and it will bring more heat energy to the rear part of weld pool, increase the volume of the weld pool, reduce the maximal temperature and finally change the isothermals.

The figures 6 and 7 show the temperature field of these two cases at the bottom surface of workpiece. In front of the heat source, the difference in the isothermals is quite small, on

the other hand, the isothermals are very different behind the heat source. The isothermals are elongated for the case with free surface than the one with fixed surface, and the temperature difference exceeds 100 K in a huge area. Therefore, it is important to consider the free surface in the simulation of GTAW process.

Table 3. Weld pool characteristics in the models with and without free surface

Model	T_{max} (K)	u_{max} ($m.s^{-1}$)	v_{max} ($m.s^{-1}$)	w_{max} ($m.s^{-1}$)	Width (mm)	Depth (mm)	Volume (mm^3)
With free surface	2486	0.31	0.32	0.15	3.60	2.36	70.6
Without free surface	2706	0.18	0.23	0.06	3.60	1.50	51.7

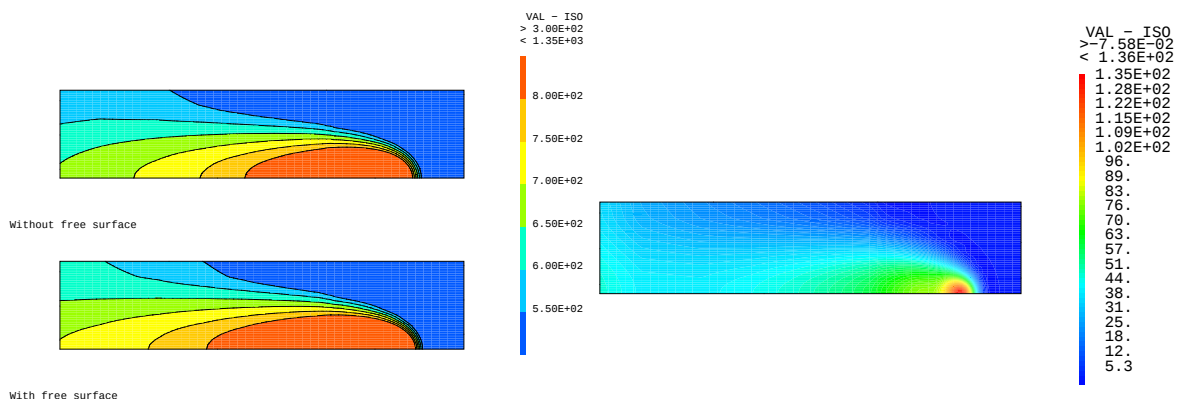


Figure 6. Calculated temperature field at the bottom surface of workpiece for the case without and with considering free surface.

Figure 7. Difference of calculated temperature field at the bottom surface of workpiece with and without considering free surface.

4.2. Weld bead geometry

The crosssection macrograph of welded joint is shown in figure 8, which also indicate the calculated weld bead shape by the models with and without free surface. As shown in this figure, the width of weld pool with a flat surface is wider than experiment and the depth is smaller, on the other hand, the shape of the weld and the penetration are better predicted when we take account into the free surface. As shown in figure 4 and figure 5, fluid flow and heat are taken away from the center of weld pool to the edge, so the deepest position of the weld pool is not just below the moving heat source, but after it because of the convection. When the surface is free, the front part of weld pool is strongly depressed by the arc pressure, so the fluid velocity at the surface is bigger and more fluid flow and heat are taken to the back part of weld pool which lead to a deeper penetration. For this experiment, the heat transfer and fluid flow model with free surface is better to predict the weld bead geometry.

5. Conclusion

A three-dimensional model of heat transfer and fluid flow has been presented in this paper, which can calculate the temperature and velocity field, predict the weld pool shape and size.

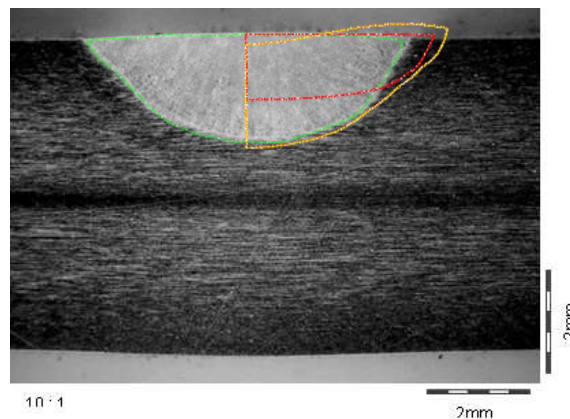


Figure 8. Experimental (green line) and calculated weld pool shape (yellow line model with free surface and red line model without free surface).

The following conclusions can be given:

- (1) The model solves the continuity, momentum conservation, and energy conservation equations with taking account into the free surface and phase change, and a steady solution for the temperature, velocity field and the free surface of weld pool can be found.
- (2) Taking account into the free surface in the simulation of weld pool has a great influence on the fluid velocity, the isothermals and the dimensions of the weld bead.
- (3) Experimental results show that there is a good agreement between the simulated profile of weld bead by our 2D-3D approach model and the experimental one.

6. Reference

- [1] Tanaka M, Terasaki H, Ushio M and Lowke J 2002 *Metallurgical and Materials Transactions A* **33** 2043–2052
- [2] Mundra K and Debroy T 1996 *Numerical Heat Transfer* **29** 115
- [3] Lu F, Tang X, Yu H and Yao S 2006 *Journal of Applied Physics* **35** 458
- [4] Wu C, Chen J and Zhang Y 2007 *Computational Materials Science* **39** 635–642
- [5] Kim J and Na S 1994 *ASME J. Eng. Ind* **116** 78–85
- [6] Hu J, Guo H and Tsai H 2008 *International Journal of Heat and Mass Transfer* **51** 2537
- [7] Brochard M 2008 *A unified model of gas tungsten arc welding including electrode, arc plasma and molten pool* Ph.D. thesis Commissariat à l’Energie Atomique, France
- [8] Cast3M 2008 <http://www-cast3m.cea.fr>
- [9] Brent A, Voller V and Reid K 1988 *Numerical Heat Transfer* **13** 297–318
- [10] Sahoo P, Debroy T and McNallan M 1988 *Metallurgy and Materials Transactions B* **19** 483–491
- [11] Nedjar B 2002 *Computers and Structures* **80** 9–21
- [12] Kim C 1975 *Thermophysical properties of stainless steels* Master’s thesis Argonne national laboratory